Applied Catalysis B: Environmental 88 (2009) 407–412

Contents lists available at ScienceDirect

Applied Catalysis B: Environmental

journal homepage: www.elsevier.com/locate/apcatb

Photodegradation of lauric acid at an anatase single crystal surface studied by atomic force microscopy

A. Zaleska [a,*], J. Nalaskowski [b], J. Hupka [a], J.D. Miller [b]

[a] Department of Chemical Technology, Gdansk University of Technology, Gdansk, Poland
[b] Department of Metallurgical Engineering, University of Utah, Salt Lake City, UT, USA

ARTICLE INFO

Article history:
Received 21 August 2008
Received in revised form 16 October 2008
Accepted 25 October 2008
Available online 6 November 2008

Keywords:
Anatase
Rutile
Single crystal
Photooxidation
AFM

ABSTRACT

The photodegradation of lauric acid at an anatase single crystal surface was visualized using atomic force microscopy (AFM). Photooxidation was performed for lauric acid thin films with thickness about 80–90 nm to simulate more realistic processing conditions rather than using submonolayer films. It was noticed that lauric acid deposited by spin coating technique formed domain structure at the TiO_2 surface. The phenomenon of domain surface decrease without change in the film thickness was observed. This suggests that only molecules at the crystal–air–lauric acid contact line and extended therefrom were degraded.

1. Introduction

Titanium dioxide is one of the most extensively studied transition metal oxides due to its availability and wide use in a variety of technological applications ranging from solar energy conversion through environmental remediation, to antibacterial, self-cleaning and antifogging functions.

Anatase, rutile and brookite are the three common crystalline polymorphs of TiO_2. Rutile is the thermodynamically most stable state (ca. 1.2–2.8 kcal mol^{-1} more stable than anatase) [1]. Anatase is stable at low-temperatures (pyramid-like crystals) and converts to rutile (needle-like) at high temperatures [1]. Anatase to rutile transformation usually occurs in the temperature range 700–1000 °C, depending on the crystallite size and impurity content. Both forms can be prepared as single crystals. The band gap energies for anatase and rutile have been estimated to be 3.2 and 3.0 eV, respectively. The smaller band gap of rutile implies that a higher fraction of solar radiation can induce band gap excitation (threefold increase in photocurrent). Titanium dioxide in the anatase form appears to be most photoactive and the most practical of the semiconductors for environmental applications.

The photochemical reaction at the surface of a TiO_2 photocatalyst is generally believed to involve radical species. Extensive studies on photooxidation of organic compounds and photodecomposition of water have provided some evidence for such intermediates [1]. However, some important issues regarding the reactive sites, the roles of individual reactant species, and the detailed reaction mechanisms remain unsettled. Single crystal surfaces provide the opportunity to study a well-defined structure with a known surface state at which surface coverage of reactant molecules and their reactivity can be controlled. Further, single crystal surfaces allow for direct observation of TiO_2 photocatalytic surface reactions using scanning probe microscopy and provide insight into the photocatalytic properties of TiO_2.

Observations of O_2 adsorption [2], formate [3] and acetate [4] decomposition, and photodecomposition of stearic acid at the surface of polycrystalline [5], and single crystal rutile [6] were performed using scanning tunneling microscopy (STM) and atomic force microscopy (AFM).

AFM has been used to study the surface structure of TiO_2 after high temperature annealing [7], the hydration of TiO_2 [8] and the photocatalytic decomposition of thin layers of organic compounds at TiO_2 surfaces. Zorbas et al. [9] used a chemically modified AFM probe to actively carry out a highly localized photochemical

* Corresponding author at: Department of Chemical Technology, Gdansk University of Technology, G. Narutowicza 11/12, 80-952 Gdansk, Poland.
Tel.: +48 58 3472437; fax: +48 58 3472065.
E-mail address: azal@chem.pg.gda.pl (A. Zaleska).

0926-3373/$ – see front matter © 2008 Published by Elsevier B.V.
doi:10.1016/j.apcatb.2008.10.020

reaction of a synthetic dye. By placing the TiO_2 powder catalyst onto the end of an AFM tip, they were able to initiate a localized photochemical reaction of a synthetic textile dye (Procion Red MX-5B) within the spatially confined region where the tip traverses, leaving the rest of the sample surface unaffected [9].

A model reaction has been employed to investigate the mechanism for the photooxidation of chlorinated hydrocarbons at rutile single crystal surface by Lu et al. [10]. They demonstrated that photooxidation of CH_3Cl on TiO_2(1 1 0) occurred only at the annealed surface in the presence of adsorbed oxygen. The oxygen vacancies are Ti^{3+} point defects which are generated by eliminating surface oxygen atoms by thermal desorption. It was found also, that adsorbed water molecules participated in the photoreaction in the presence of adsorbed molecular oxygen, leading to a formaldehyde product.

Sawunyama et al. [6] studied the nature and surface morphological changes associated with the photodegradation of stearic acid Langmuir–Blodgett (LB) films on rutile (1 1 0). Submonolayers of stearic acid consisted of circular domains of various sizes. They noted that there was no bulk differential reactivity at the island edges compared to their interior. This suggests that the rate of photodegradation of the stearic acid molecules is independent of their location in the island. They concluded that inhomogeneous reactivity patterns are probably a reflection of the momentary distribution of reaction centers [6].

While all investigations focused on the catalytic or photocatalytic activity at rutile single crystal surfaces, there is no data regarding anatase––the more active form of TiO_2 in the photocatalytic reaction. In the present study photodegradation of lauric acid at the anatase single crystal surface was visualized using AFM technique for the first time. Lauric acid, one of three most widely distributed saturated fatty acids found in the nature, was chosen as a model pollutant for the photodegradation study. The recent uses of lauric acid are in the manufacture of soaps, shampoos and other surface active agents, including lubricants. Lauric acid is an analogue of stearic acid which was used in an earlier investigation [6].

We have investigated photooxidation of organic thin films (about 80–90 nm) to simulate more realistic processing conditions rather than using submonolayer films. AFM observation of the surface morphology of thin films provided further insight into the reactivity of molecules in different regions of the lauric acid layer.

2. Experimental

2.1. Materials and instruments

Polished rutile and anatase single crystal substrates used in this work were obtained from Commercial Crystal Laboratories, Inc., USA. Crystal dimensions were 5 mm × 5 mm × 1 mm, and 10 mm × 10 mm × 1 mm for anatase and rutile, respectively. The crystals were rinsed with ethanol, and water, and then cleaned in ozone/UV cleaner (Biorad, Inc.) prior to thin film deposition. Lauric acid (99%) and acetone (analytical grade) from Sigma–Aldrich Co. were used without further purification.

The single crystal structure was determined from the XRD pattern measured in the range of $2\theta = 20$–80° using an X-ray diffractometer (Xpert PRO-MPD, Philips) with Cu target Kα-ray ($\lambda = 1.5404$ Å).

An ESCALAB-210 spectrometer (VG Scientific) was used for X-ray photoelectron spectroscopy (XPS) measurements with the Al Kα X-ray source operated at 300 W (15 kV, 20 mA). The spectrometer chamber pressure was about 5×10^{-9}mbar. Survey spectra were recorded for all the samples in the energy range from 0 to 1350 eV with 0.4 eV step. High resolution spectra were recorded with 0.1 eV step, 100 ms dwell time and 20 eV pass energy. A 90° take-off angle was used in all measurements. AVANTAGE data system software served for curve fitting. The background was fit using the nonlinear Shirley model. Scofield sensitivity factors and measured transmission function were used for quantification.

2.2. Thin films irradiation procedure

The thin films were deposited using the spin coating procedure (1800 min^{-1}). In this procedure 200 μl of 0.04 M lauric acid in acetone solution was spread over the crystal surface placed on a rotating disc, and dried afterwards. A Nanoscope IIIa Multimode AFM system (Veeco) was used to image changes in the topography of the lauric acid layer during UV irradiation. A liquid optic fiber with UV filter ($270\ nm < \lambda < 720\ nm$) was placed at approximately 10 mm distance from the sample mounted on the AFM stage and connected to a 175 W xenon light source (Spectra Physics). The AFM imaging was performed at room temperature using a contact mode NP silicon nitride triangular cantilever (Veeco) with spring constant $k = 0.12$ N/m. Data analysis and surface coverage was measured from topographic images using WSxM (Nanotec) software with the flooding image processing option [11].

IR spectra were obtained in the absorption mode by FT-IR spectroscopy (Thermo Electron Corporation – Nicolet 8700) using a liquid-nitrogen-cooled MCT detector. In a typical IR experiment, 64 scans were collected to give the final transmission spectrum and all spectra were recorded at a resolution of 4 cm^{-1}. For FT-IR investigation, 200 μl of 0.08 M lauric acid in acetone solution was spread over the crystal surface placed on a rotating disc. IR spectra were recorded after 10, 40, 70 and 130 min of irradiation.

3. Results and discussion

Thin films of lauric acid were deposited at the surfaces of rutile and anatase single crystals, and at a glass surface for a point of reference. The structure of single crystals was confirmed by XRD analysis, whereas the chemical composition of the surface layer was investigated by XPS. The XRD spectra and atomic composition are shown in Fig. 1 and Table 1, respectively. Both single crystals contain titanium atoms mainly as Ti^{4+} ions and a small amount of the reduced species of Ti^{3+} ions. For anatase and rutile the Ti^{4+}/Ti^{3+} ratio was 38:1 and 74:1, respectively. The carbon content in the surface layer varied from 50 to 70% probably due to impurities adsorbed at the TiO_2 surface. Under normal conditions, the surfaces of metals or metal oxides are usually covered by adsorbed

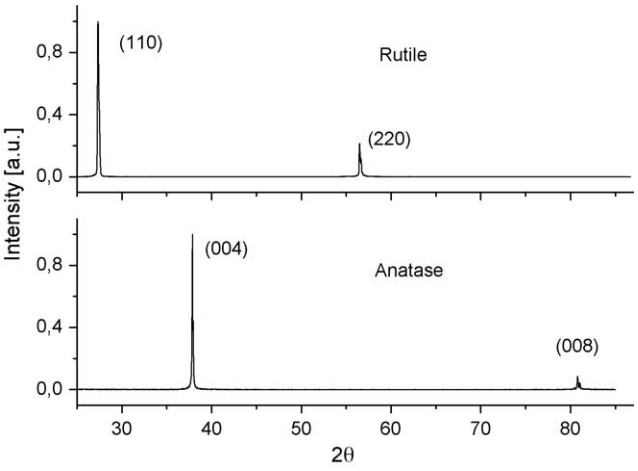

Fig. 1. XRD pattern of single crystals used in present investigation.

Table 1
Chemical composition of anatase and rutile single crystals.

TiO_2 single crystal structure	Titanium content (at.%)			Oxygen content (at.%)			Carbon content (at.%)	Nitrogen content (at.%)	Impurities (at.%)
	Ti^{4+}	Ti^{3+}	∑Ti	$O_{surf.}$	$O_{latt.}$	∑O			
Anatase	9.61	0.25	9.86	14.5	17	31.5	50.2	1.1	7.34
Rutile	5.17	0.07	5.24	11	9	20	69.7	0.6	4.46

compounds, including CO, CO_2 and hydrocarbons. Contaminants can be removed by argon etching, but the crystalline structure of the crystal surface layer could be altered by the argon ion beam.

AFM investigation demonstrated that lauric acid deposited by the spin coating method formed a relatively nonuniform layer with domain structures, as shown in Fig. 2. Domain structures are thermodynamically favorable and coalescence of the islands is a result of the minimization of surface energy through a reduction in the interfacial length of curvature [12]. Circular islands of stearic acid were observed by Sawunyama et al. [6] at a TiO_2(1 1 0) surface. In the Sawunyama et al. investigation, the monolayer film was prepared by the Wilhelmy plate method. Stearic acid in chloroform solution was spread over a $BaCl_2$ aqueous subphase maintained at 20 °C in a LB trough. The monolayers of stearic acid and/or barium stearate were transferred by a vertical dipping technique at 5 mm min^{-1}. The obtained island structures were perfectly circular. The smallest islands were approximately 1 μm in diameter with the larger islands having diameters over 20 μm [6].

The thickness of the lauric acid film obtained by the spin coating technique in our investigation was approximately 80–90 nm with some degree of nonuniformity. A fully extended lauric acid molecule has a chain length of 2 nm [13]. A simple calculation indicates that the film from spin coating corresponds to a minimum of 40 lauric acid molecules. Selected AFM images of the observed domain structures are presented in Fig. 2. Lauric acid formed island structures surrounded by film with defects and pits as shown in Fig. 2a or nonuniform film with slots and holes as shown in Fig. 2b and c. Light shades on the micrographs represent lauric acid domains while dark area depict TiO_2 surface. Total area of three islands shown in Fig. 2a was 109.27 μm^2 (27.32% of image area) and total length perimeters was 52.9 μm.

Experiments in which a thin film of lauric acid was deposited onto rutile and glass slides indicated lack of surface morphological changes. No degradation of lauric acid was observed even after 70 min exposure to UV. On the other hand, UV illumination of lauric acid deposited on the anatase surface resulted in domain depletion up to complete removal of the lauric acid film. The morphological changes during 28 min irradiation of the lauric acid film at the anatase surface are shown in Fig. 3. The thin film was completely removed after 31 min of irradiation.

Fig. 4 shows cross-sectional profiles of AFM images presented in Fig. 3. Prior to UV irradiation, about 75% of the surface was covered by the lauric acid film and fissures, pinholes or film defects were observed. After a few minutes of UV irradiation, the surface morphology revealed a widening of the fissures and pinholes, while the film thickness remained constant (see images in Fig. 3a–f and cross-sectional profiles in Fig. 4). Further irradiation resulted in isolated island-like structures with reduction of the island perimeter. Two isolated islands (thickness about 80–90 nm and diameter 1.6 and 0.93 μm) were still seen at the cross-section profile after almost 24 min of irradiation. It was observed that the surface of the anatase single crystal was gradually cleared of the adsorbed film, while residual islands maintained their height corresponding to the original film thickness. The mechanism of film disappearance indicated that the photoreaction was initiated at the lauric acid–TiO_2–air contact line.

The photodegradation rate of lauric acid was estimated from shrinking surface coverage expressed in percent, see Fig. 5. Surface coverage was estimated from surface topography images using WSxM software (Nanotec). A linear relation with a constant degradation rate was observed during the whole irradiation process. The average rate of domain width change was estimated to be approximately 0.3 μm min^{-1} based on the change in width of cross-sectional profiles.

A highly localized surface photocatalytic reaction was also described by Zorbas et al. [9]. By placing 120 nm-sized fines of anatase TiO_2 powder onto the end of an AFM tip, they were able to initiate a localized photochemical reaction of a synthetic textile dye within the spatially confined region of the tip traverses, leaving the rest of the sample surface unreacted. The computed first-order rate constant k for the AFM-catalyzed surface reaction was reported to be 0.0024 min^{-1}. This value was compared with the rate constant computed from experiments with suspended TiO_2 particles. The k value thereby determined for the reaction with suspended TiO_2 particles using the same dye concentration was found to be 0.0054 min^{-1} [9]. The higher value of the first-order rate constant for the suspended TiO_2 particle reaction appears to be due to the higher surface area.

The AFM study was supplemented by FT-IR investigation. FT-IR spectral changes for the photodegradation of lauric acid at the anatase surface and a spectrum of lauric acid in KBr as a reference are shown in Fig. 6a. FT-IR spectra were recorded after 10, 40, 70 and 130 min of irradiation. C–H stretching vibration in the region 3000–2840 cm^{-1}, deformation bands in the region

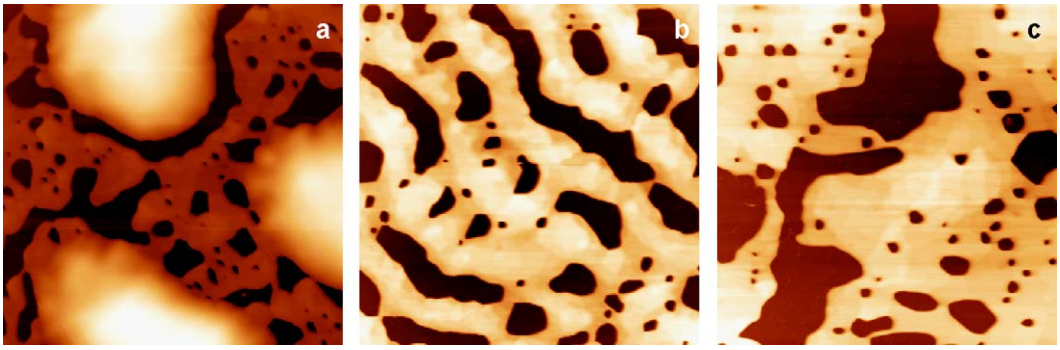

Fig. 2. AFM images of lauric acid film at an anatase single crystal surface (20 μm × 20 μm).

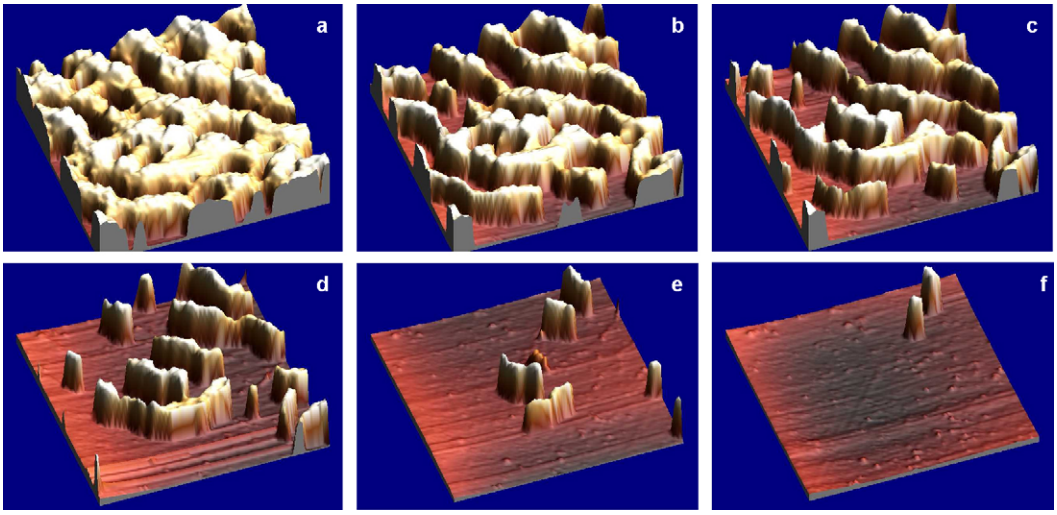

Fig. 3. Sequential AFM images (20 μm × 20 μm) of the anatase-mediated photodegradation of lauric acid film: (a) before irradiation; after (b) 11 min 40 s; (c) 16 min 20 s; (d) 21 min; (e) 25 min 40 s; (f) 28 min of irradiation.

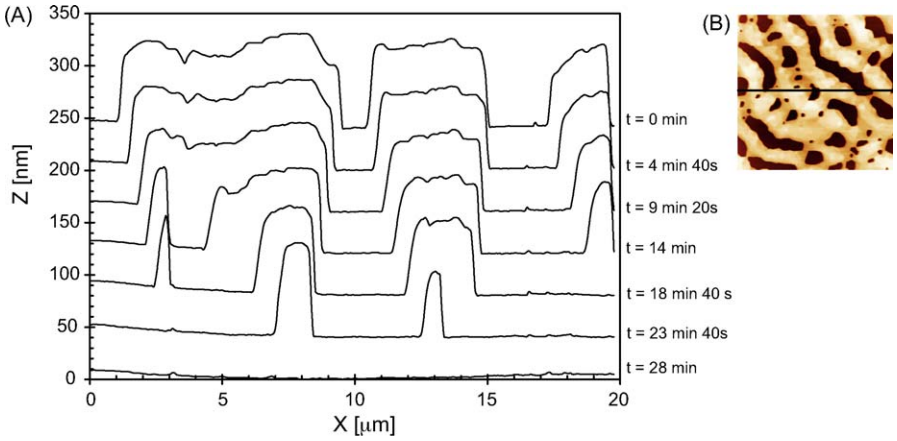

Fig. 4. Cross-sectional profiles showing the surface morphology of a thin film of lauric acid on anatase single crystal at different stages of degradation (a), AFM image (20 μm × 20 μm) showing position of cross-sectional profiles (b).

1460–1380 cm^{-1} related to CH_3– and CH_2–, and a high intensity band at about ~1700 cm^{-1}, ascribed to C=O stretching are observed. Fig. 6b and c shows the C–H stretching region and C–H vibration region. The broad absorption bands covering 960–880 cm^{-1} region are observed for the reference sample of lauric acid. Those bands are attributed to hydroxyl groups chemisorbed on the TiO_2 surface, and dissociated or molecularly adsorbed water.

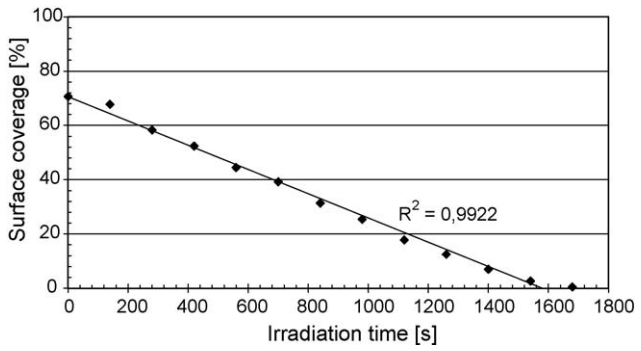

Fig. 5. Photodegradation rate of lauric acid deposited at an anatase single crystal surface.

No FT-IR spectral changes, excluding band intensity depletion, were observed during an extended irradiation. Generally, the increase in irradiation time led to reduce the intensities of the bands. By-product formation resulting in the appearance of new bands in the FT-IR spectrum was not observed. Fig. 6b and c displays changes of band intensity during irradiation for 1800–1100 and 3100–2600 cm^{-1} regions, respectively. Similar behavior was also observed by Sawunyama et al. [6] during irradiation of stearic acid at the surfaces of rutile single crystals and polycrystalline TiO_2 films.

Fig. 7 illustrates the FT-IR spectra of lauric acid before irradiation and after 130 min of irradiation at the surface of a rutile single crystal. A decrease in band intensity was not observed which is in good agreement with our previous AFM experiment.

Sawunyama et al. [6] demonstrated complete degradation of a stearic acid monolayer on a rutile single crystal surface. In our research, we did not see any degradation of the stearic acid analogue–lauric acid—at the rutile surface, while it was completely removed from anatase surface. The observed inactivity of the rutile single crystal could have resulted from lower Ti^{3+} ion concentration

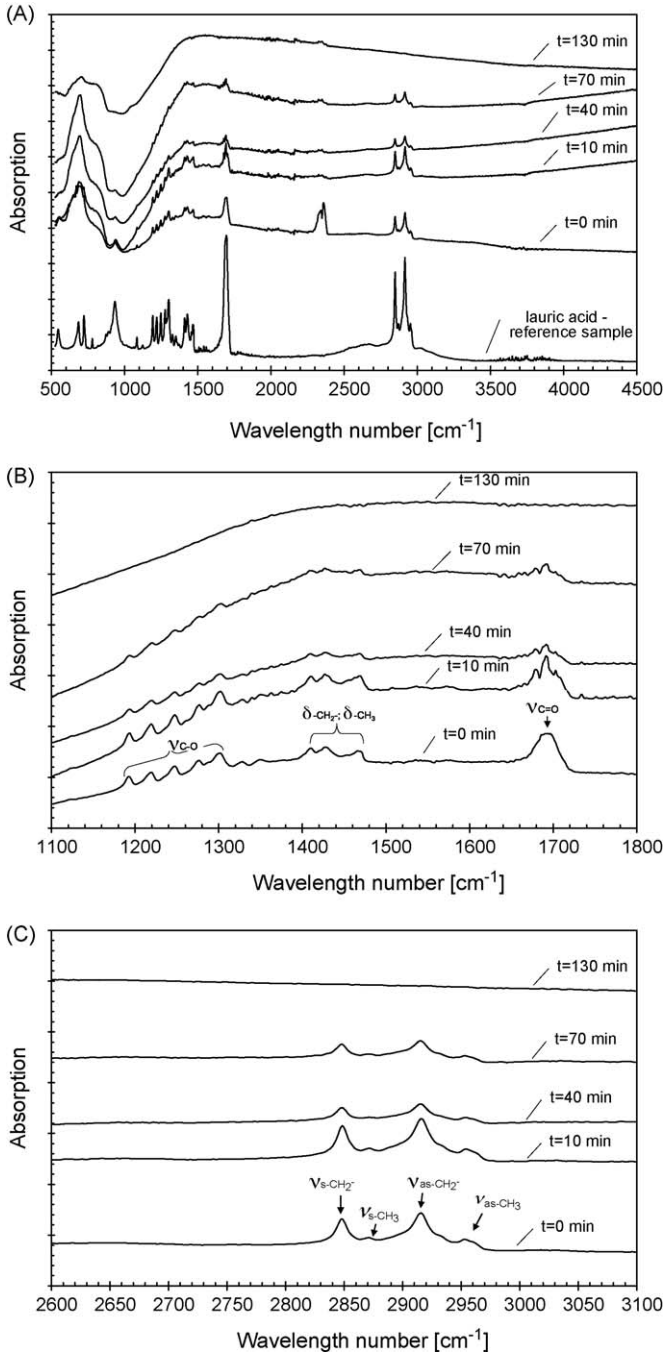

Fig. 6. Changes in FT-IR spectra during photodegradation of a thin film of lauric acid on anatase surface: (a) whole spectrum, (b) 1800–1100 cm^{-1} region and (c) 3100–2600 cm^{-1} region.

in the surface layer. Ti^{3+} ions concentration in the surface layer was 0.25 and 0.07 at.% for anatase and rutile surface, respectively, see Table 1. It was found that oxygen vacancy sites (Ti^{3+} sites) promote trapping of electrons and holes in the surface region leading to a more efficient charge transfer process. Adsorbed oxygen on the TiO_2 surface scavenges the trapped electrons, prolonging hole's lifetime and increasing the photoefficiency [10,14]. Rutile single crystals showing photoactivity [10,15] had surface defects (oxygen vacancies) produced by annealing the above surface in vacuum to 627 °C. In our investigation, anatase and rutile single crystals were used without thermal treatment, thus rutile has negligible number of surface defects resulting in lack of photoactivity.

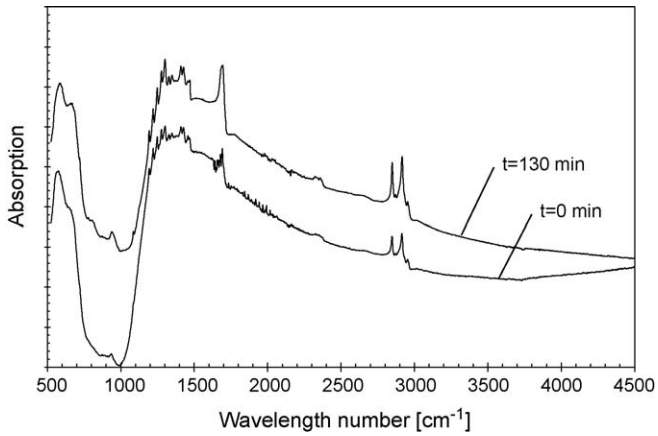

Fig. 7. Changes in FT-IR spectra during photodegradation of a thin film of lauric acid on a rutile surface.

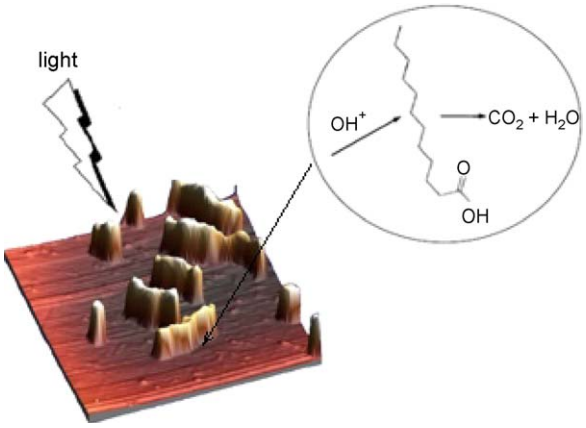

Fig. 8. Visualization of photocatalytic reaction at TiO_2–lauric acid interface.

Earlier photodegradation data reported in the literature pertain to a monolayer on a rutile single crystal [6,15,16]. In our investigation, lauric acid formed a layer over 80 nm thick, allowing for observation that the island structure thickness remained constant during photodegradation while the equivalent diameter of islands diminished. Our results suggest that the photocatalytic reaction is precisely localized at the TiO_2/lauric acid line of contact as clearly seen in Fig. 8. AFM visualization indicated that only molecules at the crystal–air–lauric acid contact line and extended therefrom were degraded.

4. Conclusions

Lauric acid forms domain structures at the surfaces of TiO_2 single crystals.

The experimental data show that the lauric acid layer was removed from the anatase single crystal surface during UV illumination. Such was not the case for the lauric acid film at the rutile single crystal surface. The anatase photoactivity most likely resulted from the presence of an oxygen vacancy.

By using organic multilayers instead of a monolayer, the importance of the TiO_2 surface role was confirmed. The phenomenon of domain surface decrease without change in the film thickness is described here for the first time. Only molecules at the crystal–air–lauric acid contact line and extended therefrom were degraded.

Acknowledgments

We acknowledge support of this work through the Seed Grant Program provided by the University of Utah, Salt Lake City, USA. Professor Janusz Strangret (Department of Physical Chemistry, Gdansk University of Technology) and Professor Maria Gazda (Department of Solid State Physics, Gdansk University of Technology) are gratefully acknowledged for assistance in ATR-IR spectroscopy and XRD analysis.

References

[1] D. Chatterjee, S. Dasgupta, J. Photochem, Photobiol. C: Photochem. Rev. 6 (2005) 186–205.
[2] H. Onishi, Y. Iwasaka, Phys. Rev. Lett. 76 (1996) 791.
[3] H. Onishi, Y. Iwasawa, Chem. Phys. Lett. 226 (1994) 111–114.
[4] H. Onishi, Y. Yamaguchi, K. Fukui, Y. Iwasaka, J. Phys. Chem. 100 (1996) 9582–9584.
[5] P. Sawunyama, L. Jiang, A. Fujishima, K. Hashimoto, J. Phys. Chem. B 101 (1997) 11000–11003.
[6] P. Sawunyama, A. Fujishima, K. Hashimoto, Langmuir 15 (1999) 3551–3556.
[7] H. Nörenberg, F. Dinelli, G.A.D. Briggs, Surf. Sci. 446 (2000) L83–L88.
[8] J.P. Bearinger, C.A. Orme, J.L. Gilbert, Surf. Sci. 491 (2001) 370–387.
[9] V. Zorbas, M. Konungo, S. Bains, Y. Mao, T. Hemray-Benny, J.A. Misewich, S.S. Wong, Chem. Commun 36 (2005) 4598–4600.
[10] G. Lu, A. Linsebigler, J.T. Yates Jr., J. Phys. Chem. 99 (1995) 7626–7631.
[11] I. Horcas, R. Fernandez, J.M. Gomez-Rodriguez, J. Colchero, J. Gomez-Herrero, A.M. Baro, Rev. Sci. Instrum. 78 (2007) 013705-1–013705-8.
[12] C.M. Knobler, Science 249 (1990) 870–874.
[13] P. Urban, B. Idzikowski, S. Kostyrya, B. Andrzejewski, Z. Vértesy, Czech. J. Phys. 54 (2004) 683–686.
[14] E. Wahlstrom, E.K. Vestergaard, R. Schaub, A. Ronnau, M. Vestergaard, E. Lægsgaard, I. Stensgaard, F. Besenbacher, Science 303 (2004) 511–513.
[15] A.L. Linsebigler, G. Lu, J.T. Yates Jr., J. Phys. Chem. 100 (1996) 6631–6636.
[16] J.C.S. Wong, A.L. Linsebigler, G. Lu, J. Fan, J.T. Yates Jr., J. Phys. Chem. 99 (1995) 335–344.